

Bounding the Effects of Continuous Treatments for Hidden Confounders

Myrl G. Marmarelis¹

Greg Ver Steeg¹

Aram Galstyan¹

¹USC Information Sciences Institute, 4676 Admiralty Way, Marina del Rey, CA 90292

Abstract

Causal inference involves the disentanglement of effects due to a treatment variable from those of confounders, observed as covariates or not. Since one outcome is ever observed at a time, the problem turns into one of predicting counterfactuals on every individual in the dataset. Observational studies complicate this endeavor by permitting dependencies between the treatment and other variables in the sample. If the covariates influence the propensity of treatment, then one suffers from *covariate shift*. Should the outcome and the treatment be affected by another variable even after accounting for the covariates, there is also *hidden confounding*. That is immeasurable by definition. Rather, one must study the worst possible consequences of bounded levels of hidden confounding on downstream decision-making. We explore this problem in the case of *continuous treatments*. We develop a framework to compute ignorance intervals on the partially identified dose-response curves, which enable us to quantify the susceptibility of our inference to hidden confounders. Our method is supported by simulations as well as empirical tests based on two observational studies.

1 INTRODUCTION

One aspect of machine learning is to build a good predictor. Another piece of the puzzle, crucial to any scientific endeavor, is to identify the causal drivers behind the predicted phenomenon. To have an *actionable* model, it is not enough to record an individual's social, lifestyle, demographic information and then correctly guess their health outcomes. The resultant model would be riddled with bias [Mehrabi et al., 2021] and unintelligible mechanisms of action, leading only to confused prescriptions. A prudent researcher would ac-

count for as many covariates as possible, and then either physically (with a Randomized Controlled Trial, or RCT) or virtually match individuals along their covariates between treatment cohorts, before drawing conclusions. Sometimes an RCT is prohibitive due to cost or ethics, e.g. forcing someone to smoke. In those cases, one must rely on observational studies and correct for confounding *post hoc*.

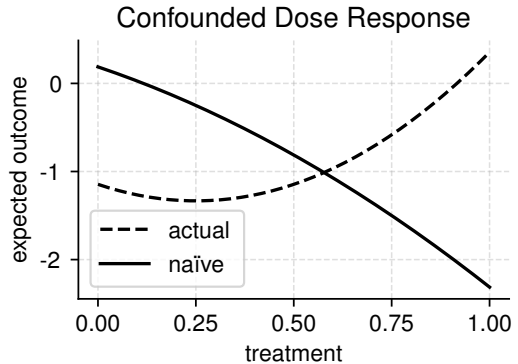


Figure 1: Hypothetical dose responses in a simplified context with continuous treatment and unobserved confounder $T, Z \in [0, 1]$, and lacking covariates. Here the conditional expected outcome $\mathbb{E}[Y|Z = z, T = t]$ is defined as $3(t - \frac{1}{4})^2 - 4z^2$ and the observations are fully confounded by the treatment regime $P(T = t|Z = z) = \delta(t - z)$. The overlap assumption for inverse propensity weighting is violated here. Still, “true” potential outcomes are revealed by forcing independence between T and Z . Then the population-wide response curve flips to face upward.

To motivate our effort, we highlight the pitfalls of a failure to incorporate possible confounding. The widely noted J-shaped curves are common in physiology [Calabrese and Baldwin, 2001]. The characteristic dynamic occurs whenever a substance in moderate concentration effects vastly different behaviors than either extremes at high or low doses. Even a trivially contrived scenario like in Figure 1 exhibits a flipping J-shaped curve due to confounding.

1.1 RELATED WORKS.

A J-shaped curve must be estimated on a continuum of treatment values. The accommodation of continuous treatments in rigorous literature has risen sharply in recent years, both in the field of econometrics (e.g. Huang et al. [2021], Tübbicke [2022]) and in machine learning (Ghassami et al. [2021], Colangelo and Lee [2021]). So far, attempts to quantify ignorance due to hidden confounding on potential outcomes have focused on the simpler case of binary treatments [Rosenbaum and Rubin, 1983]. A number of creative approaches were exhibited in the past few years to make strides in this binary setting. Most of them relied on a *sensitivity model* for bounding the extent of possible unobserved confounding, to which downstream tasks may be adapted by noting which treatment effects degrade the quickest.

Regarding binary treatments, the so-called Marginal Sensitivity Model (MSM) due to Tan [2006] continues to be studied extensively [Zhao et al., 2019, Veitch and Zaveri, 2020, Yin et al., 2021]. Variations thereof include Rosenbaum’s earlier sensitivity model [2002] that enjoys ties to regression coefficients [Yadlowsky et al., 2020]. Other groups have borrowed strategies from deep learning [Wu and Fukumizu, 2022] rather than opting for the MSM. Another active line of work constructs bounds not due to ignorance on confounding but instead viewed from the lens of robustness [Guo et al., 2022, Makar et al., 2020, Johansson et al., 2020]. The MSM is highly interpretable with its single free parameter, and applicable to a wide swath of models.

Alternative approaches to controlling for unobserved confounders require an expansion to the simple data-generating process of outcome/treatment/covariates (Y, T, X). Proximal causal learning [Tchetgen et al., 2020, Mastouri et al., 2021] loosens confounding requirements with additional proxy variables. The sensitivity analysis due to Chen et al. [2022] relies on multiple large dataset partitions.

1.2 CONTRIBUTIONS.

The MSM is incompatible with continuous treatments. Our first contribution is to propose a unique sensitivity model (§1.4) that extends the MSM to a treatment continuum. Next, we derive general formulas (§2) and specialize them to versatile closed forms (§2.2) culminating in Theorem 1. We devise an efficient algorithm (§3) to compute ignorance bounds over dose-response curves, following up with experiments on simulated (§4) and real (§5) datasets.

1.3 POTENTIAL OUTCOMES.

Causal inference is often cast in the nomenclature of potential outcomes, due to Rubin [1974]. The broad goal is to measure a treatment’s effect on an individual, demarcated by a set of covariates, while accounting for all the con-

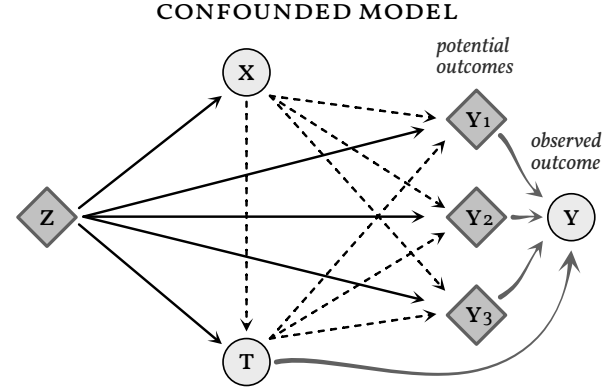


Figure 2: A simplified setting with three potential outcomes Y_1, Y_2, Y_3 arising from treatment regimes $T = 1, 2, 3$. Dashed lines represent the confounded situation wherein covariate X insufficiently captures the confounder Z behind the treatment effects. Solid lines represent the de-confounded situation, precluding any unobserved confounder, as if $X = Z$ were measured.

founding between the covariates and the treatment variable. Effects could manifest heterogeneously across individuals. In observational—i.e., not fully randomized—settings, covariates may not entirely overlap between treatment groups. It is typical to estimate two models, (1) the outcome predictor and (2) a model for the propensity of treatment conditioned on the covariates. The latter is plugged into a reweighting procedure [Reiffel, 2020] that attempts to correct for the biased treatment regimen, i.e. covariate shift, in the data.

The first two assumptions involved in Rubin’s framework are that observations of outcome, assigned treatment, and covariates $\{Y^{(i)}, T^{(i)}, X^{(i)}\}$ are i.i.d draws from the same population and that all treatments have a chance to occur for each covariate vector: $P(T = t|X = x) > 0$ (overlap/positivity) for all $t, x \in [0, 1] \times \mathcal{X}$, specifically in our context of continuous treatments. The third and most challenging of these fundamental assumptions is that of ignorability, or sufficiency. Our study is concerned with the times when that assumption is violated: when the assigned treatment statistically depends on a confounder that is not blocked by the supplied covariates. Let $p(y_t|x)$ denote the probability density function of potential outcome $Y_t = y_t$ from a treatment $t \in [0, 1]$, given covariates $X = x$. Formally, we have a violation of ignorability:

$$\{(Y_t)_{t \in \mathcal{T}} \not\perp\!\!\!\perp T\} \mid X.$$

It is only realistic to observe samples of $Y|T = t, X = x$ with density $p(y_t|t, x)$. However, to express possible hidden confounding, we also require a $p(y_t|\tau \neq t, x)$ for

$$p(y_t|x) = \int_0^1 p(y_t|\tau, x)p(\tau|x) d\tau, \quad (1)$$

where $p(y_t|\tau, x)$ is the distribution of potential outcomes conditioned on actual treatment $T = \tau \in [0, 1]$ that may differ from the potential outcome's index t . Throughout this study, y_t will indicate the value of the potential outcome at treatment t , and τ will take the place of the *other* treatment value, like the assigned treatment. For instance, we may care about the counterfactual of a smoker's ($\tau = 1$) health outcome had they not smoked ($y_{t=0}$), where $T = 0$ signifies no smoking and $T = 1$ is “full” smoking.

Interpretation. How would one interpret $p(y_t|\tau, x)$? The potential-outcomes vector $(Y_t)_{t \in [0,1]}$ of infinite dimensionality is *intrinsic* to each individual with true confounder Z , for which X is a noisy proxy. By “true” confounder we refer to any set of variables that suffice to block all backdoor paths between Y_t and T . The potential-outcomes vector would only change from knowledge of assigned treatment $T = \tau$ if it betrayed additional information about Z , absent in X , that further informed any Y_t . We may express $p(y_t|\tau, x)$ explicitly in terms of hypothetical true confounders as $\int p(y_t|z)p(z|\tau, x) dz$ because z subsumes both x and τ . This way, $p(y_t|z)$ is the true potential outcome and $p(z|\tau, x)$ acts as a filter for how parts of the true confounder mix together into the proxy x and the assigned treatment τ .

Propensities. The probability density $p(\tau|x)$ is termed the *nominal propensity*. Absent any unobserved confounding, $p(y_t|\tau, x) = p(y_t|x)$ and Equation 1 trivializes. See Figure 2 for a graphical illustration. A quantity commonly examined in the realm of causality is the *complete propensity* $p(\tau|y_t, x)$, which can differ from $p(\tau|x)$ —just like $p(y_t|\tau, x)$ from $p(y_t|x)$ —in the presence of hidden confounding. In those instances, conditioning on assigned treatment τ or potential outcome y_t modulates the distributions. It is of interest to study the impact of a bounded amount of unobserved confounding on our ignorance of $p(y_t|x)$, and the consequences on $\mathbb{E}[f(Y_t)|X]$ for various functions f .

The Marginal Sensitivity Model (MSM) serves to bound the extent of hidden confounding in the regime of binary treatments $T' \in \{0, 1\}$ [Jesson et al., 2021]. Specifically, it couples the odds of treatment under the nominal propensity to the odds of treatment under complete propensity, limiting the discrepancy to a factor Γ :

Definition 1 (The Marginal Sensitivity Model). For binary treatment $t' \in \{0, 1\}$ and violation factor $\Gamma \geq 1$,

$$\Gamma^{-1} \leq \left[\frac{p(t'|x)}{1 - p(t'|x)} \right]^{-1} \left[\frac{p(t'|y_{t'}, x)}{1 - p(t'|y_{t'}, x)} \right] \leq \Gamma.$$

Restricting ourselves to binary treatments affords us a number of conveniences. For instance, one probability value is sufficient to describe the whole propensity landscape on one set of conditions, $p(1-t'|\dots) = 1 - p(t'|\dots)$. As we transfer to the separate context of $t \in [0, 1]$, we must contend with infinite treatments and infinite potential outcomes.

1.4 TOWARDS CONTINUOUS SENSITIVITY.

We require a constraint on the fundamentally unknowable quantity $p(\tau|y_t, x)$ for any treatment $T = \tau \in [0, 1]$ and potential outcome y_t , for possibly contrary treatment assignments $\tau \neq t$. As with the MSM, our target is to associate $p(\tau|y_t, x)$ to the knowable $p(\tau|x)$. In other words, we seek to constrain the knowledge conferred on propensity by a single potential outcome y_t . It is not necessary for the functions pertaining to $(y_t)_{t \in [0,1]}$ to exhibit any degree of smoothness in t . The potential-outcome variables are treated as entries in an infinitely long vector. However, we do impose that the propensity probability densities $p(\tau|\dots)$ are at least once differentiable in τ . What sort of analogue exists for the notion of “odds” in the MSM?

Let us look to treatments τ versus $\tau + \delta$ locally, for some infinitesimal δ , at any part of the curve. A translation of the MSM might appear as

$$\left[\frac{p(\tau + \delta|x)}{p(\tau|x)} \right]^{-1} \left[\frac{p(\tau + \delta|y_t, x)}{p(\tau|y_t, x)} \right].$$

Let us peer into one of those ratios. In logarithms,

$$\delta^{-1} \log \frac{p(\tau + \delta|x)}{p(\tau|x)} = \frac{\log p(\tau + \delta|x) - \log p(\tau|x)}{\delta} \xrightarrow{\delta \rightarrow 0} \frac{\partial \log p(\tau|x)}{\partial \tau} \triangleq \partial_\tau \log p(\tau|x).$$

Hence, we introduce the notion of an infinitesimal MSM, the δ MSM, bounding $|\partial_\tau \log p(\tau|y_t, x) - \partial_\tau \log p(\tau|x)|$.

Definition 2 (The Infinitesimal Marginal Sensitivity Model). For continuous $t \in [0, 1]$ and violation factor $\Gamma \geq 1$,

$$\left| \partial_\tau \log \frac{p(\tau|y_t, x)}{p(\tau|x)} \right| \leq \log \Gamma.$$

We crafted the δ MSM with the intention of functionally mirroring the MSM—locally, on a treatment continuum. Whereas Definition 2 is stated in logarithms, Definition 1 is not; the difference is merely cosmetic and hyperparameter Γ plays an equivalent role in both structures. Nevertheless, the emergent properties are vastly different.

2 THE FRAMEWORK

We list the core assumptions surrounding our problem.

Assumption 1 (Bounded Hidden Confounding). We invoke the δ MSM of Definition 2.

Assumption 2 (Fully Observed Confounding at No Treatment). The utter lack of treatment should not be informed by potential outcomes: $p(\tau = 0|y_t, x) = p(\tau = 0|x)$ for all t and y_t .

Assumption 2 is necessary for our derivations, and yet we also argue that it is well-founded. We frame the special cohort at $T = 0$ as a control group; in a practical sense, we expect a dramatically lessened vulnerability to hidden confounders for the well-represented—in observed attributes *and* unobserved—control group. There is no additional constraint, besides the δ MSM itself, on how much the complete propensity function may fluctuate around any $T > 0$, no matter how close to zero. We motivate this assumption in the empirical case study of §5 as well.

Next, we proceed with derivations. The key to cracking open Equation 1 is to approximate $p(y_t|\tau, x)$ around $\tau = t$, where $p(y_t|t, x) = p(y|t, x)$ can be learned with any predictive model from the data on hand. However, even $\partial_\tau p(y_t|\tau, x)|_{\tau=t}$ is intractable.

2.1 AN UNRELIABLE APPROXIMATION.

Suppose that $p(y_t|\tau, x)$ is twice differentiable almost everywhere in τ . We construct a Taylor expansion

$$p(y_t|\tau, x) = p(y_t|t, x) + (\tau - t)\partial_\tau p(y_t|\tau, x)|_{\tau=t} + \frac{(\tau - t)^2}{2}\partial_\tau^2 p(y_t|\tau, x)|_{\tau=t} + \mathcal{O}(\tau - t)^3. \quad (2)$$

Denote with $\tilde{p}(y_t|\tau, x)$ an approximation of first or second order as laid out above. We choose to quantify the reliability of this approximation by a set of weights $0 \leq w_t(\tau) \leq 1$, where typically (but need not necessarily) $w_t(t) = 1$. Decompose the integral of Equation 1—

$$\begin{aligned} p(y_t|x) &= \int_0^1 w_t(\tau)p(y_t|\tau, x)p(\tau|x) d\tau \\ &\quad + \int_0^1 [1 - w_t(\tau)]p(y_t|\tau, x)p(\tau|x) d\tau \\ &\approx \int_0^1 \underbrace{w_t(\tau)\tilde{p}(y_t|\tau, x)p(\tau|x)}_{(A)} d\tau \\ &\quad + \int_0^1 \underbrace{[1 - w_t(\tau)]p(\tau|y_t, x)p(y_t|x)}_{(B)} d\tau. \end{aligned} \quad (3)$$

This separation into known (A) and unknown (B), modulated by the weights, ensures that the inaccurate regimes of the approximation vanish and are replaced with the ignorant quantity. We simplify part B of Equation 3 first:

$$\begin{aligned} \int_0^1 [1 - w_t(\tau)]p(\tau|y_t, x)p(y_t|x) d\tau \\ = p(y_t|x) \left[1 - \int_0^1 w_t(\tau)p(\tau|y_t, x) d\tau \right]. \end{aligned}$$

We witness already that $p(y_t|x)$ shall take the form of

$$p(y_t|x) \approx \frac{\int_0^1 w_t(\tau)\tilde{p}(y_t|\tau, x)p(\tau|x) d\tau}{\int_0^1 w_t(\tau)p(\tau|y_t, x) d\tau}. \quad (4)$$

To proceed further demands reflecting on the consequences of Assumptions 1 & 2. Without loss of generality, consider

$$\begin{aligned} \partial_\tau \log p(\tau|y_t, x) &= \partial_\tau \log p(\tau|x) + \gamma(\tau|y_t, x), \\ |\gamma(\tau|y_t, x)| &\leq \log \Gamma. \end{aligned} \quad (5)$$

We may attempt to integrate both sides...

$$\begin{aligned} \int_0^{t'} \partial_\tau \log p(\tau|y_t, x) d\tau &= \int_0^{t'} \partial_\tau \log p(\tau|x) d\tau \\ &\quad + \underbrace{\int_0^{t'} \gamma(\tau|y_t, x) d\tau}_{\triangleq \lambda(t'|y_t, x)} \\ \iff \log p(\tau = t'|y_t, x) - \log p(\tau = 0|y_t, x) &= \log p(\tau = t'|x) - \log p(\tau = 0|x) + \lambda(t'|y_t, x), \\ \log p(\tau|y_t, x) &= \log p(\tau|x) + \lambda(\tau|y_t, x) \\ &\quad \text{(by Assumption 2).} \end{aligned}$$

$$\therefore p(\tau|y_t, x) = p(\tau|x)\Lambda(\tau|y_t, x), \quad \Lambda \triangleq \exp\{\lambda\}. \quad (6)$$

Clearly, $|\lambda(\tau|y_t, x)| \leq \tau \log \Gamma$ and subsequently $\Lambda(\tau|y_t, x)$ is bounded by $\Gamma^{\pm\tau}$. We are now equipped with the requisite tools to properly bound $p(y_t|x)$ —or an approximation thereof, erring on ignorance via reliability weights $w_t(\tau)$. The full derivation may be found in §A.

Predicting potential outcomes. Of particular note is our recovery of a fully normalized probability density $\tilde{p}(y_t|x)$ that may be approximated with Monte Carlo or solved in closed form with specific formulations for the weights and propensity. Generally, it takes on the form $\tilde{p}(y_t|x) = d(t|y_t, x)^{-1}p(y_t|t, x)$, with

$$\begin{aligned} d(t|y_t, x) &\triangleq \mathbb{E}_\tau[\Lambda(\tau|y_t, x)] - (\gamma\Lambda)(t|y_t, x)\mathbb{E}_\tau[\tau - t] \\ &\quad - \frac{1}{2}((\dot{\gamma} + \gamma^2)\Lambda)(t|y_t, x)\mathbb{E}_\tau[(\tau - t)^2], \end{aligned} \quad (7)$$

where said expectations, $\mathbb{E}_\tau[\cdot]$, are with respect to the implicit distribution $q(\tau|t, x) \propto w_t(\tau)p(\tau|x)$.

To make use of this formula, one first procures the set of admissible $d(t|y_t, x) \in [\underline{d}(t|y_t, x), \bar{d}(t|y_t, x)]$ that violate ignorability up to a factor Γ according to the δ MSM. Then, considering their reciprocals as importance weights [Tokdar and Kass, 2010], tight bounds on the partially identified expectations over $\tilde{p}(y_t|x)$ may be optimized.

Bootstrapping over ensembles. One could exploit the parcelization of $\tilde{p}(y_t|x)$ into a predictor $p(y_t|t, x)$ as the numerator and a nominal propensity model $p(\tau|x)$ in the denominator. Should models be learned in ensembles, as in our experiments, it would be appropriate to quantify empirical uncertainties [Jesson et al., 2020] alongside robustness to hidden confounding. One way to achieve that is by bootstrap resampling [Lo, 1987] the ensembles and marginalizing over them in each part of the fraction.

2.2 TRACTABLE WEIGHTS AND PROPENSITIES.

In addition to developing the general framework above, we derive analytical forms for a specific parametrization to the weighting function and propensity distribution. Here, we look to the Beta function and its associated probability density for viable solutions. Suppose that

$$(T|X = x) \sim \text{Beta}(\alpha(x), \beta(x)), \\ \text{for arbitrary } \alpha(x), \beta(x), \quad (8)$$

$$w_t(\tau) = \frac{\tau^{a_t-1}(1-\tau)^{b_t-1}}{c_t} = \frac{\tau^{rt}(1-\tau)^{r(1-t)}}{c_t}, \\ a_t + b_t = r + 2, \quad r > 0. \quad (9)$$

The reliability weights, which we have complete freedom to design, take on the form of an unnormalized Beta density in this case. Say that $w_t(\tau)$ should peak at $\tau = t$, and that $w_t(\tau) = 1$. Immediately we can solve for $c_t \triangleq t^{rt}(1-t)^{r(1-t)}$, even though it will turn out irrelevant for our purposes. We do set the mode to t :

$$\frac{a_t - 1}{a_t + b_t - 2} = t.$$

Further, we eliminate the remaining degree of freedom by imposing a precision constraint $a_t + b_t - 2 = r$ for some $r > 0$. Constraining a more complex dispersion statistic like variance would prove much more difficult.

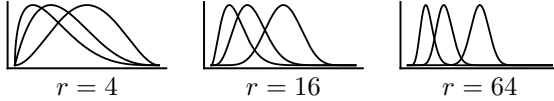


Figure 3: Beta weight schemes $w_t(\tau)$ in the unit square, plotted for centers $t = 0.125, 0.25, 0.5$. Shapes are symmetrical about $t = 0.5$. Trust declines with r .

Here, the expectations found in Equation 7 are available in closed form, and can be bounded in terms of the predictive models and just two more free parameters, Γ and r . Guidance on setting the violation factor Γ is discussed elsewhere, e.g. §5; as for the class of weights, high r conveys poor trust in the Taylor-series approximation in Equation 2, and bears the potential to widen ignorance bounds.

The findings. We pose a third and final assumption, which enables us to state Theorem 1. The main insight to unlocking those expectations is that each one of them involves an integral with the product $w_t(\tau)p(\tau|x)$, which yields an unnormalized Beta distribution. So we use the moments of that Beta distribution.

Assumption 3 (Second-order Simplification). The quantity $\dot{\gamma}(\tau|y_t, x)$ cannot be characterized as-is. We grant that γ^2 dominates over the former, and consequently

$$(\dot{\gamma} + \gamma^2)\Lambda \approx \gamma^2\Lambda.$$

Theorem 1 (Beta Parametrizations). *The formulations in Equations 8 & 9 admit analytical solutions to the ignorance denominator in Equation 7.*

$$\mathbb{E}_\tau[\Lambda(\tau|y_t, x)] \in \\ {}_1F_1(\alpha(x) + a_t - 1; \alpha(x) + \beta(x) + r; \pm \log \Gamma),$$

where again the operator \mathbb{E}_τ is employed as in Equation 7, and ${}_1F_1$ denotes Kummer's confluent hypergeometric function [Mathews Jr. et al., 2021]. In addition, with α, β implicitly referring to $\alpha(x), \beta(x)$,

$$\mathbb{E}_\tau[\tau - t] = \frac{(1-t)\alpha - t\beta}{\alpha + \beta + r},$$

$$\mathbb{E}_\tau[(\tau - t)^2] = \left[(\alpha + \beta + r)(\alpha + \beta + r + 1) \right]^{-1} \\ \cdot \left[(\alpha^2 + \beta^2 + \alpha + \beta - r)t^2 \right. \\ \left. - (2\alpha^2 + 2\alpha\beta + 2\alpha - r)t + (\alpha + 1)\alpha \right].$$

To take these findings one step further, we compare any weighting function $w_t(\tau)$ to a baseline or phantom Beta scheme with relatively low r .

Proposition 2 (Absolute Accuracy). *Suppose that*

1. $\partial_\tau^2 p(y_t|\tau, x)$ is Q -Lipschitz, and that
2. the compound propensity-weights $w_t(\tau)p(\tau|x)$ and $w_t(\tau)p(\tau|y_t, x)$ are bounded on both sides by a phantom Beta scheme, of the form in Equation 9 with narrowness r^* , up to a margin of $c^* \geq 1$.

More specifically by the second item,

$$w_t^*(\tau)/c^* \leq \{w_t(\tau)p(\tau|x), w_t(\tau)p(\tau|y_t, x)\} \leq c^* w_t^*(\tau).$$

Then the outcome approximator $\tilde{p}(y_t|x)$ of second order (Equation 7) has an absolute error stemming from the Taylor remainder on $p(y_t|\tau, x)$, stated in terms of these constants:

$$|p(y_t|x) - \tilde{p}(y_t|x)| \leq (c^*)^2 (r^* + 1) k(r^*) Q.$$

The unitless $k(r^*)$, pertaining to the numerator in Equation 4, was solved numerically for certain values of r^* :

r^*	0.5	1	2	4
$(r^* + 1) k(r^*)$	0.03	0.02	0.01	0.005

Pertinent to the above result is the tendency for compound propensity-weights $w_t(\tau)p(\tau|x)$ to be narrower than the weights $w_t(\tau)$ themselves. This holds especially in the Beta family of propensities, per the discussion surrounding Equation 8. See §B for more details on the proposition.

3 COMPUTING THE IGNORANCE INTERVALS

We are interested in characterizing $\mathbb{E}[f(Y_t)|X = x]$ for any $f(y)$ that suits a downstream task. We accomplish this by implementing a Monte Carlo importance sampler with n outcome realizations y_i drawn from proposal $q(y)$:

$$\tilde{\mathbb{E}}[f(Y_t)|X = x] = \frac{\sum_{i=1}^n f(y_i)\tilde{p}(y_t = y_i|x)/q(y_i)}{\sum_{i=1}^n \tilde{p}(y_t = y_i|x)/q(y_i)}. \quad (10)$$

Even though $\tilde{p}(y_t|x)$ is a normalized probability density, it contains partially identified quantities. It is untenable to constrain a search along the assignments for $d(t|y_t = y_i, x)$ to even approximately ensure $\int_{\mathcal{Y}} \tilde{p}(y_t = y|x) dy = 1$. For this reason the bias of an estimator without the corrective denominator of Equation 10 would be uncontrollable [Todor and Kass, 2010]. A greedy algorithm may be deployed to maximize $\tilde{\mathbb{E}}[f(Y_t)|X = x]$ in this form by using weights

$$\underline{w}_i := \frac{p(y_i|t, x)}{d(t|y_i, x)q(y_i)}, \quad \overline{w}_i := \frac{p(y_i|t, x)}{\bar{d}(t|y_i, x)q(y_i)}.$$

The minimum may be achieved by a trivial extension. Maximizing and minimizing $\tilde{\mathbb{E}}[f(Y_t)|X = x]$ with respect to the bounding quantities (γ, Λ) enables the resolution of ignorance bounds on the basis of Γ from Definition 2.

Our algorithm, displayed below, adapts the method of Jesson et al. [2021] to heterogeneous weight bounds $[\underline{w}_i, \overline{w}_i]$ per draw i . View a proof of correctness in §C.

input : $\{(\underline{w}_i, \overline{w}_i, f_i)\}_{i=1}^n$ ordered by ascending f_i .
output : $\max_w \mathbb{E}[f(X)]$ estimated by importance sampling with n draws.

Initialize $w_i \leftarrow \overline{w}_i$ for all $i = 1, 2, \dots, n$;

for $j = 1, 2, \dots, n$ **do**

 Compute $\Delta_j \triangleq \sum_{i=1}^n w_i(f_j - f_i)$;

if $\Delta_j < 0$ **then**

$w_j \leftarrow \underline{w}_j$;

else

 break;

end

end

Return $\sum_i w_i f_i / \sum_i w_i$;

Algorithm 1: The expectation maximizer, with $\mathcal{O}(n)$ runtime if intermediate Δ_j results are memoized.

4 A SYNTHETIC EXPERIMENT

We first study an idealized scenario with one hidden confounder and no covariate shift. In our design choices we sought simplicity, inducing a complicated enough dose-response function that varies with (x, t) , and a true propensity $T|Z$ that deliberately obeys Assumption 2. The piecewise

uniform distribution below has valid categorical probabilities assigned to each “bucket” that sum to unit and remain in the unit interval. The arbitrary coefficients were concocted prior to any experimentation. As for covariates, z_1 passed through entirely and z_2 remained hidden.

1,500 training and 500 testing examples were generated. We trained ensembles of eight neural networks with two hidden layers of 16 units, for the Bernoulli predictor and Beta propensity each.

$$\begin{aligned} Z = (Z_1, Z_2) &\sim \text{i.i.d Unif}(0, 1) \\ (T|Z = z) &\sim \begin{cases} \text{U}(0, 0.2) & \text{w.p } 0.1 \\ \text{U}(0.2, 0.5) & \text{w.p } 0.4 - 0.2z_2 \\ \text{U}(0.5, 0.7) & \text{w.p } 0.3 + 0.3z_2 \\ \text{U}(0.7, 0.8) & \text{w.p } 0.1 - 0.1z_2 \\ \text{U}(0.8, 1) & \text{w.p } 0.1 \end{cases} \\ (X|Z = z) &\sim \text{Dirac}(z_1) \\ (Y|T = t, Z = z) &\sim \text{Bernoulli}(z_1^{1-z_2} t^{z_2}) \end{aligned} \quad (11)$$

In reality, an unconfounded ground truth—like the black line in Figure 5—would stay unobserved. This instance, however, lends us special tools for model evaluation. Uncertainty of an ignorance interval $[\underline{y}, \bar{y}]$ with respect to a true Bernoulli(y^*) outcome was measured in an information-theoretic way. We calculated for every (t, x) the expression $\int_{\underline{y}}^{\bar{y}} \text{KL}_B(y^*||y) dy$, where KL_B is shorthand for the KL-divergence between two Bernoulli variables with the given probabilities, true y^* and inferred y .

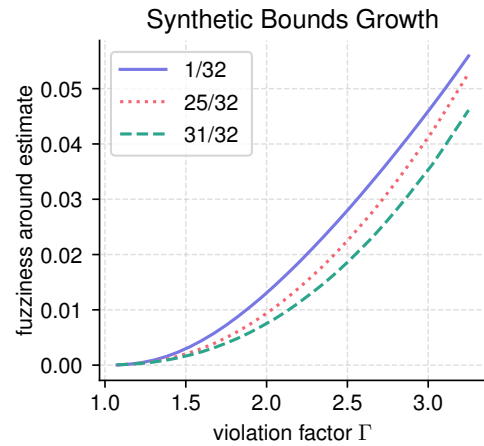


Figure 4: Uncertainty due to ignorance bounds from the δMSM with increasing Γ , in the synthetic world described by Equations 11. Representative parts of the covariate space $X = 1/32, 25/32, 31/32$ are plotted. The takeaway is that uncertainty grows faster at the individuals where treatment effect is misidentified, as witnessed in Figure 5.

Synthetic Treatment Effects at Individual Covariates

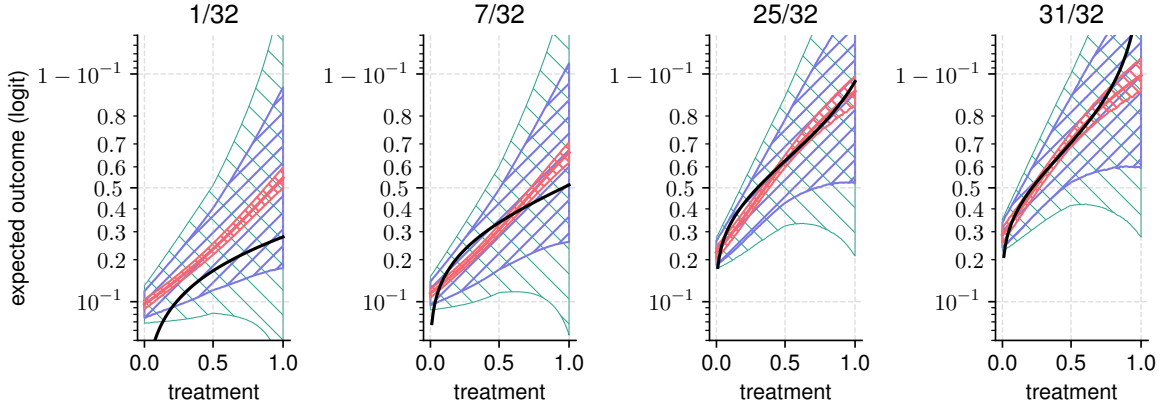


Figure 5: Continuous-treatment effects for synthetic individuals, evaluated on a grid of six covariate values $X = 1/32, 7/32, 25/32, 31/32$. Bernoulli expectations are plotted in a logit transformation because the significance of a perturbation is proportional to $y(1 - y)$. The **black line** is $p(y_t|x)$, which we get by integrating the ground truth over the real (yet unknown to the model) $p(z_2)$. Greater confounding manifests in the smaller covariates. **Red:** 95% empirical uncertainty in the model ensembles. **Blue:** ignorance + empirical interval at $r = 128$, $\Gamma = 2.125$. **Green:** $\Gamma = 3.25$.

5 RESULTS FROM AN OBSERVATIONAL STUDY

The most pertinent application for the framework laid out above is an observational study with incomplete or noisy covariates and a continuous treatment variable. More concretely, the treatment variable should be transformed and scaled into the unit interval such that $T = 0$ signifies a control with a complete lack of treatment. Every *kind* of individual should be about as likely to fall in the ($T = 0$) cohort (Assumption 2.) As for shaping the ($T > 0$) regime, the domain should inform whether a linear scale is employed, versus an empirical or parametric (i.e. standard normal) cumulative density function.

The data. We conducted two experiments, termed Drug and Vitamin, based on observational studies. The dataset for Drug consisted of self-reported drug usage and psychological state from the NSDUH in the US [Jones and Nock, 2022, James D. Sexton and Hendricks, 2020]. For Vitamin, we studied individuals from a recently published record of COVID-19 mortality from Israel, with a focus on pre-infection Vitamin D levels [Dror et al., 2022]. See §D for particulars on construction of the two datasets. A quarter of the data were reserved randomly for the test sets.

The estimators. In both experiments, the predictor and ensemble were trained as ensembles of artificial neural networks with two inner residual layers. We chose the “swish” activation function for its well-behaved gradients [Raghuram et al., 2017]. The flagship ADAM optimizer was employed for stochastic gradient descent with a learning

rate of 10^{-3} , untuned, and no mini-batching. Our analysis involved bootstrapping the ensemble to garner empirical uncertainties. For Drug, the outcome on a bounded interval was modeled as a Beta variable. The mortality outcome was Bernoulli distributed in the Vitamin model.

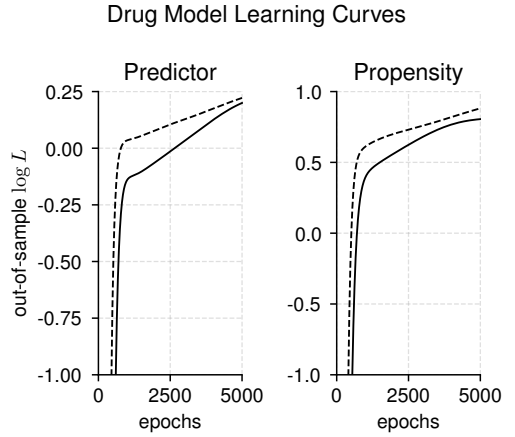


Figure 6: Learning curves of models trained on the full (**dashed**) versus censored (**solid**) drug dataset. Censoring the data does not appear to reduce the out-of-sample predictability, but it does hamper inference of the unrealized potential outcomes as witnessed in Figure 7.

Test-set log-likelihoods over the course of training are charted in Figure 6. One cannot look to predictive performance out of sample for how well the fully unconfounded dose-response curves are captured, since any hidden confounding would persist. Precise ground-truth curves can either be contrived synthetically on the basis of real covari-

ates, or garnered from a large-scale fully randomized study. A synthetic potential outcome would always carry the risk of presenting an unrealistic scenario [Curth et al., 2021].

The objective. We chose to investigate the coverage of $\mathbb{E}[Y_t|X]$ from ignorance intervals on censored covariates. This test relies on approximating an unconfounded model by collecting a large set of covariates, and then learning another model on a heavily censored version. Our reasoning is that the censored model would suffer from a greater degree of hidden confounding. The censored model could then be assessed along all potential-outcome predictions, by pretending that the full model represented the real dose-response curves. A pertinent metric would be how much a sensitivity model with $\Gamma \geq 1$ swallows the “real” dose responses, as a trade-off against the sheer area of the ignorance bounds. These competing quantities can be viewed as a form of recall and (the opposite of) precision, respectively. See Figures 7 & 8 for trade-off curves on the test set.

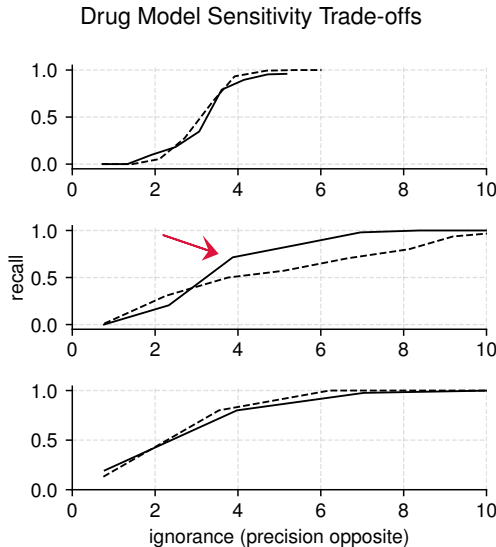


Figure 7: Fraction of the full model’s response captured by the censored model (recall), judged in terms of overlap at 95% confidence, versus the volume ratio of partial identification to full response (ignorance). The response surface was partitioned into equal thirds, *exposing a strong deviation* in the middle. **Solid:** our δ MSM with $r = 16$. **Dashed:** result of shoehorning our model into the binary MSM by triggering a binary treatment at $T > 0.5$ and discretizing the propensity by its cumulative distribution at the threshold.

6 DISCUSSION

The utility of our framework is evident in the above showcased results. We demonstrated that, in the presence of a solid ground truth (§4), the procedure discriminates between more and less confounded outcomes by selectively growing

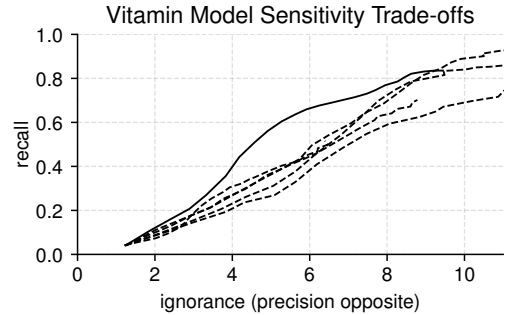


Figure 8: Ignorance versus recall, as presented in Figure 7, but for Vitamin. We compare δ MSM (**solid**) and shoehorned MSM (**dashed**) with separate lines for various T cutoffs $\{0.25, 0.33, 0.50, 0.67, 0.75\}$. Here $r = 32$ (not 16) to allow higher Γ with non-vacuous bounds.

the ignorance bounds (Figure 4). The role of the learned propensity model $p(\tau|x)$ is critical in that operation.

With the real datasets (§5), we analyzed how the heavily confounded (censored) model recovered the less confounded (full) model’s full array of potential outcomes. Our main finding is that our method accomplished it more efficiently (via the trade-off curves in Figures 7 & 8), as compared to the binarized procedure invoking a prior method due to Kallus et al. [2019] and Jesson et al. [2021]. Efficiency relates to the concept of coverage [McCandless et al., 2007]. It is vital in order to facilitate subsequent decision-making.

The novel δ MSM in Definition 2 is intuitive and now supported by experimental evidence. A benefit that would be difficult to replicate is the streamlined derivations that followed directly from our sensitivity model and a couple of additional minimal assumptions.

Future work. Our scope solely considered the univariate distributions $p(y_t|x)$ for each potential outcome. It was only necessary to grapple with the complete propensity of first order, $p(\tau|y_t, x)$. In theory, there could exist more exhaustive “complete propensities” such as $p(\tau|y_{t_1}, y_{t_2}, x)$, which we term *of second order*. These high-order propensities only become relevant alongside joint distributions, like $p(y_{t_1}, y_{t_2}|x)$. It may be fruitful to study these.

7 CONCLUSION

We successfully bridged a hidden-confounding sensitivity model to continuous treatments. Our extension is parsimonious in that it imposes minimal additional requirements on the data or predictor. We carried these results into a complete pipeline for quantifying ignorance intervals on dose-response curves. Namely, we bounded the approximation error in Proposition 2 and detailed an efficient algorithm to solve the optimization via Algorithm 1. Our observational experimentation validated the method’s core assumptions.

References

Edward J Calabrese and Linda A Baldwin. U-shaped dose-responses in biology, toxicology, and public health. *Annual Review of Public Health*, 22(1):15–33, 2001. doi: 10.1146/annurev.publhealth.22.1.15. PMID: 11274508.

You-Lin Chen, Lenon Minorics, and Dominik Janzing. Correcting confounding via random selection of background variables. *arXiv preprint arXiv:2202.02150*, 2022.

Kyle Colangelo and Ying-Ying Lee. Double debiased machine learning nonparametric inference with continuous treatments. *arXiv preprint arXiv:2004.03036*, 2021.

Alicia Curth, David Svensson, Jim Weatherall, and Mihaela van der Schaar. Really doing great at estimating CATE? a critical look at ML benchmarking practices in treatment effect estimation. In *Thirty-fifth Conference on Neural Information Processing Systems Datasets and Benchmarks Track (Round 2)*, 2021.

Amiel A Dror, Nicole Morozov, Amani Daoud, Yoav Namir, Orly Yakir, Yair Shachar, Mark Lifshitz, Ella Segal, Lior Fisher, Matti Mizrachi, et al. Pre-infection 25-hydroxyvitamin d3 levels and association with severity of covid-19 illness. *Plos one*, 17(2):e0263069, 2022.

AmirEmad Ghassami, Numair Sani, Yizhen Xu, and Ilya Shpitser. Multiply robust causal mediation analysis with continuous treatments. *arXiv preprint arXiv:2105.09254*, 2021.

Wenshuo Guo, Mingzhang Yin, Yixin Wang, and Michael Jordan. Partial identification with noisy covariates: A robust optimization approach. In *First Conference on Causal Learning and Reasoning*, 2022.

Wei Huang, Oliver Linton, and Zheng Zhang. A unified framework for specification tests of continuous treatment effect models. *Journal of Business & Economic Statistics*, 0(0):1–14, 2021. doi: 10.1080/07350015.2021.1981915.

Charles D. Nichols James D. Sexton and Peter S. Hendricks. Population survey data informing the therapeutic potential of classic and novel phenethylamine, tryptamine, and lysergamide psychedelics. *Frontiers in Psychiatry*, 10 (896), 2020.

Andrew Jesson, Sören Mindermann, Uri Shalit, and Yarin Gal. Identifying causal-effect inference failure with uncertainty-aware models. *Advances in Neural Information Processing Systems*, 33:11637–11649, 2020.

Andrew Jesson, Sören Mindermann, Yarin Gal, and Uri Shalit. Quantifying ignorance in individual-level causal-effect estimates under hidden confounding. *ICML*, 2021.

Fredrik D Johansson, Uri Shalit, Nathan Kallus, and David Sontag. Generalization bounds and representation learning for estimation of potential outcomes and causal effects. *arXiv preprint arXiv:2001.07426*, 2020.

Grant M. Jones and Matthey K. Nock. Exploring protective associations between the use of classic psychedelics and cocaine use disorder: a population-based survey study. *Nature Scientific Reports*, 12(2574), 2022.

Nathan Kallus, Xiaojie Mao, and Angela Zhou. Interval estimation of individual-level causal effects under unobserved confounding. In *The 22nd international conference on artificial intelligence and statistics*, pages 2281–2290. PMLR, 2019.

Albert Y. Lo. A large sample study of the bayesian bootstrap. *The Annals of Statistics*, 15(1):360–375, 1987.

Maggie Makar, Fredrik Johansson, John Guttag, and David Sontag. Estimation of bounds on potential outcomes for decision making. In Hal Daumé III and Aarti Singh, editors, *Proceedings of the 37th International Conference on Machine Learning*, volume 119 of *Proceedings of Machine Learning Research*, pages 6661–6671. PMLR, 13–18 Jul 2020.

Afsaneh Mastouri, Yuchen Zhu, Limor Gultchin, Anna Korb, Ricardo Silva, Matt Kusner, Arthur Gretton, and Krikamol Muandet. Proximal causal learning with kernels: Two-stage estimation and moment restriction. In *International Conference on Machine Learning*, pages 7512–7523. PMLR, 2021.

Wesley N. Mathews Jr., Mark A. Esrick, ZuYao Teoh, and James K. Freericks. A physicist’s guide to the solution of kummer’s equation and confluent hypergeometric functions. *arXiv preprint arXiv:2111.04852*, 2021.

Lawrence C. McCandless, Paul Gustafson, and Adrian Levy. Bayesian sensitivity analysis for unmeasured confounding in observational studies. *Statist Med*, 26:2331–2347, 2007.

Ninareh Mehrabi, Fred Morstatter, Nripsuta Saxena, Kristina Lerman, and Aram Galstyan. A survey on bias and fairness in machine learning. *ACM Computing Surveys (CSUR)*, 54(6):1–35, 2021.

Prajit Ramachandran, Barret Zoph, and Quoc V. Le. Searching for activation functions. *arXiv preprint arXiv:1710.05941*, 2017.

James A Reiffel. Propensity score matching: The ‘devil is in the details’ where more may be hidden than you know. *The American Journal of Medicine*, 133(2):178–181, 2020.

P. R. Rosenbaum. *Observational Studies*. Springer, 2002.

P. R. Rosenbaum and D. B. Rubin. Assessing sensitivity to an unobserved binary covariate in an observational study with binary outcome. *Journal of the Royal Statistical Society Series B (Methodological)*, 45(2):212–218, 1983.

D. B. Rubin. Estimating causal effects of treatments in randomized and nonrandomized studies. *Journal of Educational Psychology*, 66(5):688, 1974.

Zhiqiang Tan. A distributional approach for causal inference using propensity scores. *Journal of the American Statistical Association*, 101(476):1619–1637, 2006.

Eric J Tchetgen Tchetgen, Andrew Ying, Yifan Cui, Xu Shi, and Wang Miao. An introduction to proximal causal learning. *arXiv preprint arXiv:2009.10982*, 2020.

Surya T. Tokdar and Robert E. Kass. Importance sampling: A review. *WIREs Computational Statistics*, 2(1):54–60, 2010.

Stefan Tübbicke. Entropy balancing for continuous treatments. *J Econ Methods*, 11(1):71–89, 2022.

Victor Veitch and Anisha Zaveri. Sense and sensitivity analysis: Simple post-hoc analysis of bias due to unobserved confounding. In H. Larochelle, M. Ranzato, R. Hadsell, M. F. Balcan, and H. Lin, editors, *Advances in Neural Information Processing Systems*, volume 33, pages 10999–11009. Curran Associates, Inc., 2020.

Pengzhou Abel Wu and Kenji Fukumizu. β -intact-VAE: Identifying and estimating causal effects under limited overlap. In *International Conference on Learning Representations*, 2022.

Steve Yadlowsky, Hongseok Namkoong, Sanjay Basu, John Duchi, and Lu Tian. Bounds on the conditional and average treatment effect with unobserved confounding factors. *arXiv preprint arXiv:1808.09521*, 2020.

Mingzhang Yin, Claudia Shi, Yixin Wang, and David M. Blei. Conformal sensitivity analysis for individual treatment effects. *arXiv preprint arXiv:2112.03493v2*, 2021.

Qingyuan Zhao, Dylan S. Small, and Bhaswar B. Bhattacharya. Sensitivity analysis for inverse probability weighting estimators via the percentile bootstrap. *Journal of the Royal Statistical Society (Series B)*, 81(4):735–761, 2019.

A ADDITIONAL DERIVATIONS

Consider Equation 3.A:

$$\begin{aligned}
\int_0^1 w_t(\tau) \tilde{p}(y_t|\tau, x) p(\tau|x) d\tau &= \underbrace{p(y_t|t, x) \int_0^1 w_t(\tau) p(\tau|x) d\tau}_{(A.0)} \\
&+ \underbrace{g_1(y_t|t, x) \int_0^1 w_t(\tau)(\tau-t) p(\tau|x) d\tau}_{(A.1)} + \underbrace{g_2(y_t|t, x) \int_0^1 w_t(\tau) \frac{(\tau-t)^2}{2} p(\tau|x) d\tau}_{(A.2)},
\end{aligned}$$

where $g_k(y_t|t, x) \triangleq \partial_\tau^k p(y_t|\tau, x)|_{\tau=t}$. (12)

Lightening the notation with a shorthand for the weighted expectations, $\langle \cdot \rangle_\tau \triangleq \int_0^1 w_t(\tau)(\cdot)p(\tau|x) d\tau$, it becomes apparent that we must grapple with the pseudo-moments $\langle 1 \rangle_\tau$, $\langle \tau - t \rangle_\tau$, and $\langle (\tau - t)^2 \rangle_\tau$. Note that t should not be mistaken for a “mean” value.

Furthermore, we have yet to fully characterize $g_k(y_t|t, x)$. Observe that

$$p(y_t|\tau, x) = \frac{p(\tau|y_t, x)p(y_t|x)}{p(\tau|x)} \iff \partial_\tau p(y_t|\tau, x) = p(y_t|x) \cdot \frac{\partial}{\partial \tau} \frac{p(\tau|y_t, x)}{p(\tau|x)}.$$

The $p(y_t|x)$ will be moved to the other side of the equation as needed; by Equation 6,

$$\frac{\partial}{\partial \tau} \frac{p(\tau|y_t, x)}{p(\tau|x)} = \frac{\partial}{\partial \tau} \Lambda(\tau|y_t, x).$$

Expanding,

$$\begin{aligned}
&= \frac{\partial}{\partial \tau} \exp \left\{ \int_0^\tau \gamma(\tau|y_t, x) d\tau \right\} = \gamma(\tau|y_t, x) \exp \left\{ \int_0^\tau \gamma(\tau|y_t, x) d\tau \right\} \\
&= (\gamma \Lambda)(\tau|y_t, x).
\end{aligned}$$

Appropriate bounds will be calculated for $g_2(y_t|t, x)$ next, utilizing the finding above as their main ingredient. Let

$$\tilde{g}_k(y_t|t, x) \triangleq p(y_t|x)^{-1} g_k(y_t|t, x) = \left(\frac{\partial}{\partial \tau} \right)^k \frac{p(\tau|y_t, x)}{p(\tau|x)} \Big|_{\tau=t}.$$

The second derivative may be calculated in terms of the ignorance quantities γ, Λ :

$$\begin{aligned}
\tilde{g}_2(y_t|t, x) &= \partial_\tau \gamma(\tau|y_t, x) \Lambda(\tau|y_t, x) \\
&= \gamma(\tau|y_t, x)^2 \Lambda(\tau|y_t, x) + \dot{\gamma}(\tau|y_t, x) \Lambda(\tau|y_t, x) \\
&= (\gamma^2 + \dot{\gamma}) \Lambda(\tau|y_t, x).
\end{aligned}$$

And finally we address $\tilde{p}(y_t|x)$. Carrying over the components of Equation 12 into Equation 3,

$$\begin{aligned}
\tilde{p}(y_t|x) &= \frac{p(y_t|t, x) \langle 1 \rangle_\tau}{\langle \Lambda(\tau|y_t, x) \rangle_\tau - \tilde{g}_1(y_t|t, x) \langle \tau - t \rangle_\tau - \tilde{g}_2(y_t|t, x) \langle (\tau - t)^2 \rangle_\tau} \\
&= \frac{p(y_t|t, x)}{\mathbb{E}_\tau[\Lambda(\tau|y_t, x)] - (\gamma \Lambda)(t|y_t, x) \mathbb{E}_\tau[\tau - t] - \frac{1}{2}((\dot{\gamma} + \gamma^2) \Lambda)(t|y_t, x) \mathbb{E}_\tau[(\tau - t)^2]},
\end{aligned} \tag{13}$$

where these expectations $\mathbb{E}_\tau[\cdot]$ are with respect to the implicit distribution $q(\tau|t, x) \propto w_t(\tau)p(\tau|x)$. The first term in the denominator, $\mathbb{E}_\tau[\Lambda(\tau|y_t, x)]$, may be approximately bounded by the same Algorithm 1.

B DETAILS ON PROPOSITION 2

The numerics were accomplished via Wolfram Mathematica 12. Our steps for calculating key quantities are listed below.

Firstly, since the second derivative employed in the Taylor expansion is Q -Lipschitz, we have $|\partial_\tau^3 p(y_t|\tau, x)| \leq Q$. Let us denote the Taylor remainder in this scope as $\rho(y_t|\tau, x)$. By Taylor's theorem,

$$|\rho(y_t|\tau, x)| \leq \frac{|\tau - t|^3}{6} Q.$$

We carry over the remainder into the formulation of $\tilde{p}(y_t|x)$ as in Equation 4, reproduced more explicitly below.

$$\tilde{p}(y_t|x) = \frac{\int_0^1 w_t(\tau) [p(y_t|\tau, x) + \rho(y_t|\tau, x)] p(\tau|x) d\tau}{\int_0^1 w_t(\tau) p(\tau|y_t, x) d\tau}$$

By acknowledging that an exact approximation requires $\rho(y_t|\tau, x) = 0$, we express the absolute error in our imperfect approximator as

$$|\tilde{p}(y_t|x) - p(y_t|x)| = \left| \frac{\int_0^1 w_t(\tau) \rho(y_t|\tau, x) p(\tau|x) d\tau}{\int_0^1 w_t(\tau) p(\tau|y_t, x) d\tau} \right| \leq \frac{\left| \int_0^1 c^* w_t^*(\tau) \rho(y_t|\tau, x) d\tau \right|}{\int_0^1 w_t(\tau) p(\tau|y_t, x) d\tau}.$$

We analytically solved the definite integral $\int_0^1 c^* w_t^*(\tau) \frac{1}{6} Q |\tau - t|^3 d\tau \geq \left| \int_0^1 c^* w_t^*(\tau) \rho(y_t|\tau, x) d\tau \right|$, bounding the numerator. We omitted the full expansion for brevity. Then, for specific values of r^* as displayed in the table of the theorem statement, we maximized the quantity numerically over the support $0 \leq t \leq 1$ in order to obtain $k(r^*)$.

Next, on reducing the denominator, we employed the opposite side of our bound:

$$\int_0^1 w_t(\tau) p(\tau|y_t, x) d\tau \geq \frac{1}{c^*} \int_0^1 w_t^*(\tau) d\tau = \frac{B(tr^* + 1, (1-t)r^* + 1)}{c^* t^{tr^*} (1-t)^{(1-t)r^*}}.$$

The resultant fraction is symmetric about $t = \frac{1}{2}$. We posit—for it was too unwieldy to prove—that the expression is concave in $t \in [0, 1]$ for all $r^* > 0$. We validated this claim by testing the non-positivity of the second derivative at relevant values of r^* across the domain in t . It follows that the fraction achieves its minimum at the boundaries $t = 0, 1$. In either of those cases it may be evaluated by means of the identity $B(r^* + 1, 1) = (r^* + 1)^{-1}$. Hence, we assert that the above fraction is no lesser than $[c^*(r^* + 1)]^{-1}$.

Regardless of the validity of the above conjecture, the quantities displayed in the table of Proposition 2 are correct because the relation surely holds at those points in r^* .

C CORRECTNESS OF ALGORITHM 1

The algorithm functions by incrementally reallocating mass (relative, in the weights) to the righthand side, from a cursor beginning on the lefthand side of the “tape”.

Proof. Firstly we characterize the indicator quantity Δ_j . Differentiate the quantity to be maximized with respect to w_j ;

$$\begin{aligned} \frac{\partial}{\partial w_j} \frac{\sum_i w_i f_i}{\sum_i w_i} &= \frac{f_j}{\sum_i w_i} - \frac{\sum_i w_i f_i}{(\sum_i w_i)^2} \\ &= \frac{f_j \sum_i w_i - \sum_i w_i f_i}{(\sum_i w_i)^2} \\ &\propto \underbrace{\sum_i w_i (f_j - f_i)}_{\triangleq \Delta_j} \quad \text{up to some positive factor.} \end{aligned}$$

Hence, Δ_j captures the sign of the derivative.

We shall proceed with induction. Begin with the first iteration, $j = 1$. No weights have been altered since initialization yet. Therefore we have

$$\Delta_1 = \sum_i \bar{w}_i (f_1 - f_i).$$

Since $\forall i, f_1 \leq f_i$ due to the prior sorting, Δ_1 is either negative or zero. If zero, trivially terminate the procedure as all function values are identical.

Now assume that by the time the algorithm reaches some $j > 1$, all $w_k = \underline{w}_k$ for $1 \leq k < j$. In other words,

$$\Delta_j = \sum_{i < j} \underline{w}_i \underbrace{(f_j - f_i)}_{(+)} + \sum_{i > j} \bar{w}_i \underbrace{(f_j - f_i)}_{(-)}.$$

Per the algorithm, we would flip the weight $w_j \leftarrow \underline{w}_j$ only if $\Delta_j < 0$. In that case,

$$\sum_{i < j} \underline{w}_i (f_j - f_i) < \sum_{i > j} \bar{w}_i (f_i - f_j), \quad \text{where both sides are non-negative.}$$

Notice that the above is not affected by the current value of w_j . This update can only increase the current estimate because the derivative remains negative and the weight at j is non-increasing. We *must* verify that the derivatives for the previous weights, indexed at $k < j$, remain negative. Otherwise, the procedure would need to backtrack to possibly flip some weights back up.

More generally, with every decision for weight assignment, we seek to ensure that the condition detailed above is not violated for any weights that have been finalized. That includes the weights before j , and those after j at the point of termination. Returning from this digression, at $k < j$ after updating w_j ,

$$\Delta_k = \sum_{i \leq j} \underline{w}_i (f_k - f_i) + \sum_{i > j} \bar{w}_i (f_k - f_i).$$

To glean the sign of this, we refer to a quantity that we know.

$$\begin{aligned} &\sum_{i < j} \underline{w}_i (f_j - f_i) < \sum_{i > j} \bar{w}_i (f_i - f_j) \\ \iff &\sum_{i \leq j} \underline{w}_i (f_k - f_i) < \sum_{i > j} \bar{w}_i (f_i - f_j) + \sum_{i \leq j} \underline{w}_i (f_k - f_j) \\ \iff &\underbrace{\sum_{i \leq j} \underline{w}_i (f_k - f_i) + \sum_{i > j} \bar{w}_i (f_k - f_i)}_{\Delta_k} < \underbrace{\sum_{i > j} \bar{w}_i (f_k - f_j) + \sum_{i \leq j} \underline{w}_i (f_k - f_j)}_{\text{negative.}} \end{aligned}$$

The remaining fact to be demonstrated is that upon termination, when $\Delta_j \geq 0$, no other pseudo-derivatives $\Delta_{j'}, j' > j$ are negative. This must be the case simply because $f_{j'} \geq f_j$. \square

D EXPERIMENTAL DETAILS

Drug dataset. We elected to study self-reported data on drug use from the NSDUH in the US. These surveys, conducted between 2015–2019, have led to widely prolific population-level analyses [Jones and Nock, 2022, James D. Sexton and Hendricks, 2020]. For our purposes we focused on the few individuals that reportedly used hallucinogenic drugs within the preceding year. The “treatment” comprised their frequency, measured in days, of hallucinogenic drug use for that duration. It was transformed to a unit interval by the empirical cumulative distribution on the positive frequencies, setting aside the bulk ($T = 0$) group. Individuals’ age (six levels,) household income (four levels,) education status (five levels,) overall health assessment (four levels,) household size (six levels,) racial and gender-based demography (seven one-hot categories,) experience with marijuana (binary,) and city size (three levels) constituted the covariate vectors of fourteen dimensions in total. The outcome variable was a composite index of psychological distress, split into 24 levels, for the past year since the survey took place. Selection on the already arbitrary sample of respondents took place as follows: all 1,036 individuals reporting any hallucinogenic drug use were retained, and the rest with a 0.05 probability each, totalling 1,279 for the ($T = 0$) group. Ultimately, the sample size was 2,315. The occurrence of relevant drug users was likely confounded by a myriad of factors like social status and institutional distrust. To simulate a censored dataset, we eliminated the household size, demography, and marijuana usage variables.

Vitamin dataset. The data acquired from Dror et al. [2022] included 253 individuals, with 38 deaths attributed to COVID-19. The full set of recorded covariates were gender (two categories,) age (three levels,) body-mass index (two levels,) religion (five categories,) and six binary-labeled comorbidities. Vitamin D levels, the treatment variable, were scaled to the unit interval such that “healthy” levels of at least 40 ng/mL were allocated to $T = 0$ and T increased to 1 linearly as vitamin levels tended to zero. The censored dataset omitted the religion and comorbidity categories.

Drug estimators. Both the predictor and the propensity model, censored and uncensored, were trained in ensembles of 32 artificial neural networks with two inner residual layers of 16 activation units each. A dropout of 0.05 was imposed on these layers. Since both the outcome and the treatment variables were graded in a bounded interval, both models learned to parametrize a Beta distribution.

Vitamin estimators. The inner predictor- and propensity-model layers comprised four activation units each, owing to the smaller set of covariates. The dropout was increased to 0.1. The smaller models were trained in ensembles of 64 in this case.

E SOURCE-CODE AVAILABILITY

Please visit <https://github.com/marmarelis/TreatmentCurves.jl>.